Mon. Not. R. Astron. Soc. **331,** 169–179 (2002)

The evolving accretion disc in the black hole X-ray transient XTE J1859+226

R. I. Hynes,★[1] C. A. Haswell,[2] S. Chaty,[2] C. R. Shrader[3] and W. Cui[4]

[1]*Department of Physics and Astronomy, University of Southampton, Southampton SO17 1BJ*
[2]*Department of Physics and Astronomy, The Open University, Walton Hall, Milton Keynes MK7 6AA*
[3]*Laboratory for High-Energy Astrophysics, NASA Goddard Space Flight Center, Greenbelt, MD 20771, USA*
[4]*Department of Physics, Purdue University, 1396 Physics Building, West Lafayette, IN 47907-1396, USA*

Accepted 2001 November 16. Received 2001 November 14; in original form 2001 September 13

ABSTRACT

We present *HST*, *RXTE*, and UKIRT observations of the broad-band spectra of the black hole X-ray transient XTE J1859+226 during the decline from its 1999–2000 outburst. Our UV spectra define the 2175-Å interstellar absorption feature very well and based on its strength we estimate $E(B-V) = 0.58 \pm 0.12$. Hence we deredden our spectra and follow the evolution of the spectral energy distribution on the decline from outburst. We find that the UV and optical data, and the X-ray thermal component when detectable, can be fitted with a simple blackbody model of an accretion disc heated by internal viscosity and X-ray irradiation, and extending to close to the last stable orbit around the black hole, although the actual inner radius cannot be well constrained. During the decline we see the disc apparently evolving from a model with the edge dominated by irradiative heating towards one where viscous heating is dominant everywhere. The outer disc radius also appears to decrease during the decline; we interpret this as evidence of a cooling wave moving inwards and discuss its implications for the disc instability model. Based on the normalization of our spectral fits we estimate a likely distance range of 4.6–8.0 kpc, although a value outside this range cannot securely be ruled out.

Key words: accretion, accretion discs – binaries: close – stars: individual: XTE J1859+226.

1 INTRODUCTION

Black hole X-ray transients (BHXRTs), also referred to as X-ray novae and soft X-ray transients, are low-mass X-ray binaries in which long periods of quiescence, typically decades, are punctuated by very dramatic X-ray and optical outbursts, often accompanied by radio activity (Tanaka & Shibazaki 1996; Cherepashchuk 2000). In a typical outburst, the X-ray emission is dominated by thermal emission from the hot inner accretion disc, and UV, optical, and IR emission is thought to be produced by reprocessing of X-rays, predominantly by the outer disc. Studies of the UV–IR can thus tell us about the structure of the outer disc and the effect of irradiation upon it.

XTE J1859+226 was discovered on 1999 October 9 by the All Sky Monitor (ASM) of the *Rossi X-Ray Timing Explorer* (*RXTE*) (Wood et al. 1999). A 15th magnitude optical counterpart was identified by Garnavich, Stanek & Berlind (1999). Wagner et al. (1999) provided spectroscopic confirmation, finding a spectrum typical of BHXRTs in outburst. The source was also detected in the radio (Pooley & Hjellming 1999) and γ-ray (McCollough & Wilson 1999; dal Fiume et al. 1999) bands. Subsequent observations of the $R \sim 23$ quiescent optical counterpart have confirmed an orbital period of ~9.1 h (Garnavich & Quinn 2000; Sanchez-Fernandez et al. 2000; Filippenko & Chornock 2001) and a radial velocity analysis has yielded an exceptional mass function of $f(M) = (7.4 \pm 1.1)\,M_\odot$ (Filippenko & Chornock 2001), one of the largest amongst the BHXRTs. This makes it one of the most securely identified Galactic black holes.

During the outburst a series of coordinated *HST*, *RXTE* and UKIRT observations were made. The times of the observations are marked above the *RXTE*/ASM light curve in Fig. 1. Some of the results on X-ray timing have already been presented by Cui et al. (2000). A more thorough analysis of the outburst light curves and variability will be presented by Ioannou et al. (in preparation). A further work will discuss the emission-line spectrum and detailed X-ray spectral modelling. Here we focus on the evolution of the ultraviolet–optical–infrared (UVOIR) spectral energy distribution (SED) and the implied evolution of the accretion disc.

2 OBSERVATIONS

2.1 *HST* observations

HST observations of XTE J1859+226 were made using the Space

★E-mail: rih@astro.soton.ac.uk

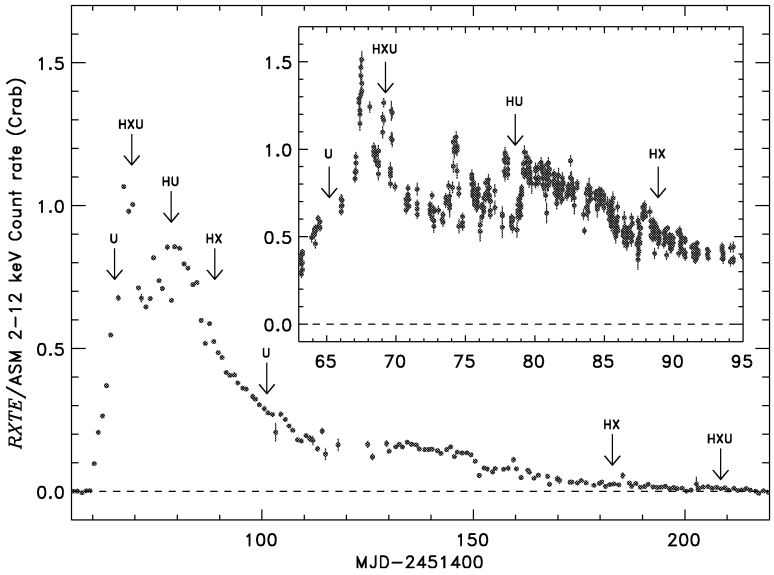

Figure 1. *RXTE*/ASM light curve of XTE J1859+226 in outburst based on quick-look results provided by the ASM/*RXTE* team. The main figure shows one-day averages of the whole period we cover; the inset shows individual 90-s dwells from the early flaring period. Times of observations are marked with arrows, annotated H (*HST*), X (*RXTE*) and/or U (UKIRT).

Table 1. Log of *HST*/STIS observations of XTE J1859+226.

Date	Start time (UT)	Exp. time (s)	Grating
1999 Oct 18	02:19:14	2250	G140L
	03:41:40	2300	G230L
	05:18:42	2300	G140L
	06:05:57	250	G230L
	06:55:22	300	G430L
	07:06:47	200	G750L
	08:32:06	2300	G140L
1999 Oct 27	19:55:24	2250	G140L
	21:20:00	1350	G140L
	21:52:16	300	G430L
	22:03:41	203	G750L
	22:57:02	2300	G230L
1999 Nov 6	19:57:20	2200	G230L
	21:21:59	850	G140L
	21:44:17	400	G430L
	21:57:22	659	G750L
2000 Feb 8	17:19:52	1500	G140L
	18:31:16	1150	G140L
	19:00:12	450	G430L
	19:14:07	253	G750L
	20:08:38	2800	G140L
	21:44:57	2800	G230L
	23:21:55	2800	G140L
2000 Mar 5	06:39:52	1500	G140L
	07:53:57	960	G140L
	08:19:43	450	G430L
	08:33:38	250	G750L
	09:31:15	2760	G140L
	11:07:32	2760	G230L
	12:44:26	2760	G140L

Telescope Imaging Spectrograph (STIS; Leitherer et al. 2001) in five visits spanning 1999 October 18 to 2000 March 5. Unfortunately no observations were obtained between 1999 November 5 and 2000 February 8 owing to an *HST* gyro failure and the target's proximity to the Sun. At each epoch we obtained full but not simultaneous wavelength coverage from 1150 to 10 200 Å using the G140L and G230L MAMA modes and the G430L and G750L CCD modes. A large aperture (52×0.5 arcsec^2) was used to ensure photometric accuracy. Full details are given in Table 1.

To examine the target's SED we used one-dimensional spectra from the standard pipeline data products. The photometric calibration accuracy is estimated at 4 per cent for MAMA modes and 5 per cent for CCD modes (Leitherer et al. 2001). There is a further uncertainty in matching different spectra owing to source variability between exposures.

We constructed a continuum SED by masking out all significant emission and absorption features (interstellar features were identified with the aid of Blades et al. 1988) and then binning to $\Delta\log\nu = 0.01$ for the first three visits and $\Delta\log\nu = 0.02$ for the two later ones. As the pipeline did not remove all cosmic rays from CCD data, we took the median of all continuum points within the bin for these data. For MAMA data a straight average was taken. A further complication is that G750L data suffer from significant fringing above ~8300 Å, even though contemporaneous flat fields were taken. This is averaged out within the bins, however.

2.2 *RXTE* observations

We observed XTE J1859+226 with the *RXTE* proportional Counter Array (PCA) and High-Energy Timing Experiment (HEXTE) at various epochs selected to coincide with the *HST* visits. Results presented here are from two specific epochs at which well-characterized thermal X-ray components are seen; 1999 October 18 (observation ID 40122-01-01-03) and 1999 November 6 (observation ID 40122-01-03-01). We have not included analysis of the HEXTE data or later visits here, since these do not contribute to our modelling of the accretion disc emission. The source intensity was about 2400 and 800 count s^{-1} per PCU at the respective epochs, and the exposure times were 3100 and 1600 s. We used the standard-2 data (128 spectral channels, 16-s accumulations), selecting sub-intervals when the number of

detectors on remained constant (about 90 per cent of the total time) to form 128-channel detector count spectra. A subset of these channels, corresponding to about 3–20 keV, were used in subsequent model fitting. Background rates were estimated using the epoch-4 models, and response matrices were generated using the current calibration files and response-matrix generation software, all from the HEASOFT 5.1 release.

The ~3–20 keV SEDs are suggestive of a high–soft state (i.e. high $\dot{m}$) accreting black hole, in that they consist of a thermal disc component with a characteristic energy of about 1 keV, superimposed on a power law, probably formed by Comptonization, with index $\Gamma \simeq 2.5$, extending to higher energies. However, the ratio of the power law to disc components appears to be relatively high for the first observation. The Galactic hydrogen column density is not well constrained by these data, and it was assumed to be in the range of about $0.3–0.8 \times 10^{22}$ cm^{-2} (Markwardt, Marshall & Swank 1999; dal Fiume et al. 1999), i.e. it was treated as a variable parameter of our fitting, but constrained to that approximate range. Fitting the data to a disc–blackbody model plus a power law leads to values of $kT_{\rm in} \simeq 1.1$ and 0.9 keV and $\Gamma \simeq 2.5$ and 1.9 at the two successive epochs. This hardening of the power-law component is suggestive of the onset of a transition towards the low–hard state. Indeed, some spectra from the later epochs of our campaign are consistent with a low–hard-state source, with no discernible disc contribution.

2.3 UKIRT observations

Near-infrared service observations of XTE J1859+226 were carried out at the United Kingdom Infrared Telescope (UKIRT) 3.8-m telescope using the 1024×1024 pixel UFTI (1–2.5 μm) camera (pixel scale 0.09 arcsec) between 1999 October 14 (Chaty et al. 1999) and 2000 March 5. The broad band filters J (1.17–1.33 μm), H (1.49–1.78 μm) and K (2.03–2.37 μm) were used. The conditions were photometric for most of the observations, the seeing being typically 0.8 arcsec. A full log of the results is given in Table 2.

Each exposure of the object is the average of 1-min integration time frames, repeated nine times by offseting the images by 1 arcmin to the north-west, north-east, south-east and south-west from the central position. The final image is constructed by coadding and median-filtering those individual frames. Total exposure times were therefore 9 min in each filter. The images were processed using IRAF reduction software. Each of the images was corrected by a normalized flat field, and sky-subtracted using a sky image created by combining with a median filter a total of nine consecutive images. The data were then analysed using the IRAF reduction task APPHOT, taking different apertures depending on the photometric conditions.

Absolute photometry was performed using a nearby NICMOS photometric standard star from the new system of faint near-infrared standard stars (Persson et al. 1998): HST 9177 (P182-E), with exposures of J, H and K (5 alternate images of 15 s for each filter). We also used the UKIRT Faint Standard FS30 (Casali & Hawarden 1992; Hawarden et al. 2001).

3 CORRECTION FOR INTERSTELLAR EXTINCTION

To determine the intrinsic SED of the source it is necessary to correct for interstellar extinction. For a review of the problem see Fitzpatrick (1999; hereafter F99). This correction is especially important, and problematic, in the vacuum UV. Here the extinction is largest, but also most uncertain, as there is significant variance between UV extinction curves along different lines of sight; see Fitzpatrick & Massa (1990) for a compilation of examples. In correcting spectral energy distributions we would ideally like to know the 'true' extinction curve for the line of sight to the target, but this is usually not known; instead it is common to assume some average Galactic extinction curve, e.g. Seaton (1979). A somewhat more sophisticated approach is to select from a family of generic extinction curves, parametrized by $R_V = A_V/E(B-V)$, based on the properties of the line of sight (e.g. diffuse gas or dense cloud); the extinction curves of Cardelli, Clayton & Mathis (1989) and F99 adopt this approach. If R_V is not known, however, it is necessary to assume some average value, usually taken to be $R_V = 3.1$. As we have no independent information on the properties of the interstellar medium towards XTE J1859+226, we adopt the F99 $R_V = 3.1$ extinction curve as this should be the 'best' current Galactic average curve. In analysing our results we must then remember that our uncertainties depend not only on the uncertain amount of extinction but the uncertain shape of the extinction curve.

To estimate the amount of extinction parametrized by $E(B-V)$, we measure the strength of the 2175 Å interstellar absorption feature. This approach has previously been used on the BHXRTs X-ray Nova Muscae 1991 (Cheng et al. 1992), GRO J0422+32 (Shrader et al. 1994) and GRO J1655–40 (Hynes et al. 1998) as well as on other classes of objects. In fitting the feature we must assume some underlying spectral shape, either fixed or with some free parameters, and then adjust $E(B-V)$ to fit the data. For XTE J1859+226 we began by fitting a reddened power law to the data with the spectral index and normalization of the power law adjusted to give the best fit for a given $E(B-V)$. We measure the badness-of-fit of a particular model by the χ^2 statistic of a fit to either the whole G230L spectrum (averaged over the first three visits with spectral features masked out) or to a subset of this. The results of this power-law fitting are summarized in Table 3 and two examples are plotted in Fig. 2(a). Clearly fitting the whole spectral range yielded a rather poor fit with χ^2_R, the χ^2 per degree of freedom, quite high. Using a more restricted range over which the spectral shape will be dominated by the profile of the 2175-Å feature rather than the shape of the underlying spectrum gives a

Table 2. Results from UKIRT/UFTI observations of XTE J1859+226.

Date	JD	J	H	K
1999 Oct 14	2451465.69	14.508 ± 0.011	14.231 ± 0.014	13.833 ± 0.013
1999 Oct 18	2451469.69	–	–	14.516 ± 0.012
1999 Oct 27	2451478.69	15.080 ± 0.015	14.689 ± 0.010	14.469 ± 0.023
1999 Nov 19	2451501.69	15.504 ± 0.008	15.232 ± 0.009	15.033 ± 0.025
2000 Mar 5	2451609.17	17.240 ± 0.029	16.935 ± 0.027	16.673 ± 0.029

Table 3. Summary of results of fitting G230L spectra with reddened models.

Model	Fit range (Å)	$E(B-V)$	χ^2_R
Power law	1650–3120	0.56	1.74
	1650–2500	0.59	1.28
	1900–3120	0.57	1.70
	1900–2500	0.59	1.21
Irradiated disc	1650–3120	0.58	1.24
	1650–2500	0.60	1.18
	1900–3120	0.58	1.26
	1900–2500	0.60	1.20

better fit but a similar $E(B-V)$ value. For all the fits considered here the statistical errors in $E(B-V)$ are tiny, $\sigma_{E(B-V)} \lesssim 0.01$, so the dominant uncertainties are systematic. Dereddening the SED with $E(B-V) = 0.58$ (Fig. 3) it is clear why the fit to the whole G230L spectrum is poor; the underlying spectrum does not appear to be a power law, but instead is curved in $\log \nu - \log F_\nu$ space. As discussed in Section 4, a simple irradiated disc spectrum provides a good empirical description of the SEDs from the early visits. We therefore repeat the fitting using such a model for the underlying spectrum, allowing the normalization and edge temperature to vary to give the best fit for each $E(B-V)$. The fits, also summarized in Table 3 and illustrated in Fig. 2(b), are better than with a power law, even when the whole G230L spectrum is used, but the derived $E(B-V)$ values are similar. Hence the derived reddening is

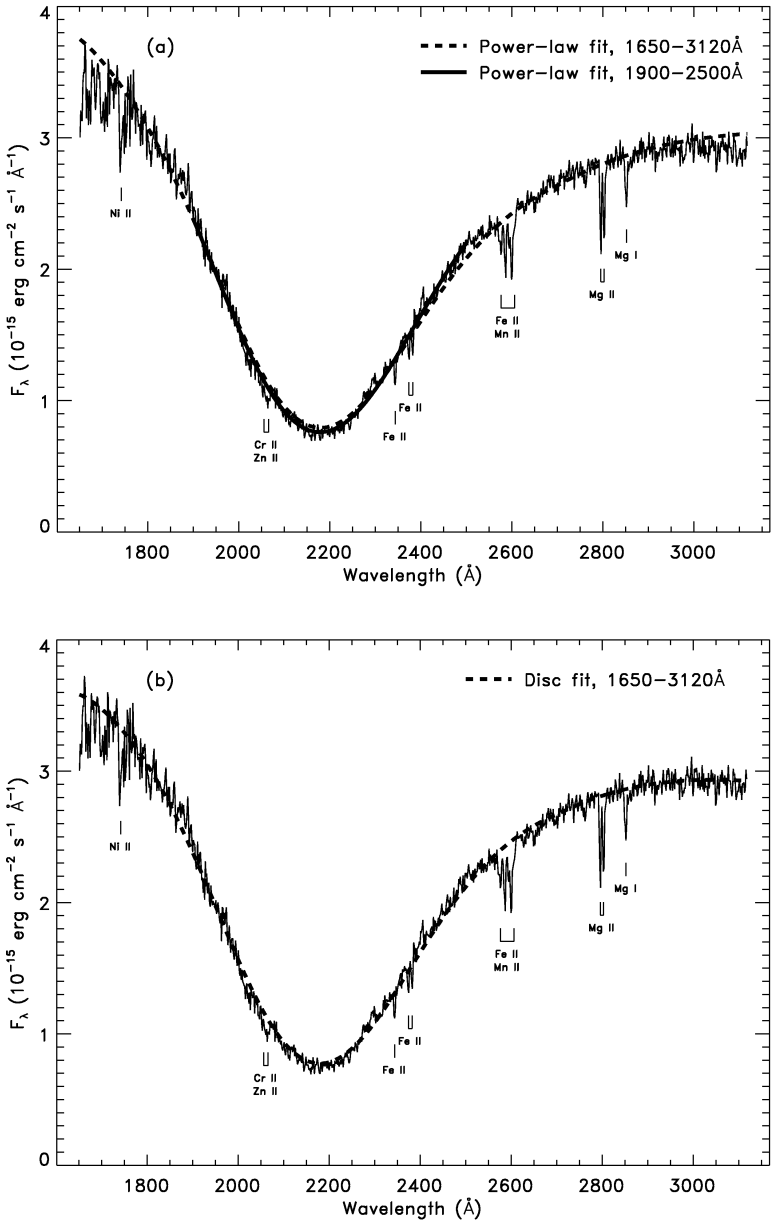

Figure 2. (a) Fit to G230L spectrum using reddened power-law models. Two fits are shown, using wide and narrow spectral regions. The former is clearly a poor fit. (b) Fit using an irradiated disc model. This fit is good, except at the shortest wavelengths where the extinction curve may be incorrect. In both cases the significant interstellar absorption lines are marked; these were masked out before doing the fit.

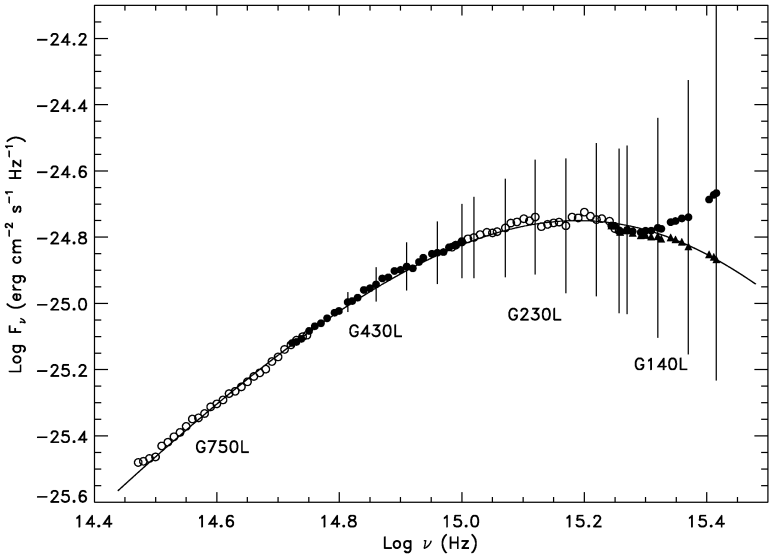

Figure 3. Average spectral energy distribution from the first three visits dereddened assuming a F99 Galactic average extinction curve with $E(B-V)=0.58$. Error bars on every fifth UV point indicate the uncertainty introduced by intrinsic variance of extinction curves from average, following the treatment in F99. Alternate solid and filled circles are used to distinguish the different gratings. The solid triangles indicate the G140L spectrum dereddened with the modified extinction curve described in the text. The model overplotted is an irradiated disc model, as described in the text, with $T_{\rm out}=18\,000$ K.

relatively insensitive to the both the assumed spectral model and the exact wavelength range fitted. The dominant uncertainty is caused by the variation in strength of the 2175-Å feature, relative to $E(B-V)$, between different lines of sight, about 20 per cent (F99). Our preferred value is based on fitting the whole G230L spectrum with an irradiated disc model. This provides a reasonable fit and the value derived, 0.58, conveniently lies fairly central within the spread of inferred values, 0.56–0.60. Our estimate of the reddening, accounting for possible variation of the strength of the 2175-Å feature from average is then $E(B-V)=0.58\pm0.12$.

We show in Fig. 3 the average spectrum from the first three visits. This has been dereddened assuming the F99 extinction curve with $E(B-V)=0.58$. We overplot a pure irradiated disc model (see Section 4) for comparison, with the irradiation temperature inferred from the fit to the G230L spectrum. Clearly the model provides an extremely good fit to most of the SED, even in the optical region which was not explicitly fitted. The only major deviation is in the far-UV, where the abrupt upturn is difficult to explain. This is in the place where a deviation would be expected if the far-UV rise component of the extinction is somewhat different to the Galactic average; this can vary independently of other parts of the extinction curve, and is only weakly correlated with the strength of the 2175-Å feature (Fitzpatrick & Massa 1988; F99). The far-UV rise is also the component which differs most between different estimates of the Galactic average extinction curve (F99). To test this we modify the F99 average curve by changing the far-UV rise parameter, c_4. We find that if we use $c_4=0.25$ instead of the average value of $c_4=0.41$ then the far-UV spectrum does fit the model very well. $c_4=0.25$ is well within the range observed in individual line-of-sight extinction curves (Fitzpatrick & Massa 1990), so this is a plausible interpretation. We also note that if the SED is dereddened using the Seaton (1979) extinction curve, for the same value of $E(B-V)$, then the fit to the irradiated disc model in the far-UV is rather good (e.g. Hynes & Haswell 2001). The deviation from the average F99 curve is thus not only within the spread observed in single stars, but within the range of independent estimates of the true Galactic average curve. We therefore believe that the most likely reason for the poor fit in the far-UV is that the extinction curve is not quite that of F99. For modelling in Section 4 we therefore perform two sets of fits. Our preferred approach is to fit the whole dataset using the F99 average curve except for taking $c_4=0.25$. To test the sensitivity to the far-UV extinction uncertainty we also fit using an unmodified F99 curve and exclude the G140L data.

4 SPECTRAL MODELLING

4.1 The model

To fit the broad-band SED we use a very simple parametrized model. This is based on a combination of the classic viscously heated black body disc spectrum (Shakura & Sunyaev 1973; Frank, King & Raine 1992) and the modified temperature distribution for an irradiated disc (Cunningham 1976; Vrtilek et al. 1990). See these papers for derivations of the relevant temperature distributions, and Dubus et al. (1999) for a critique of the assumptions.

The model spectrum is calculated by summing a series of black bodies over radius. The local effective temperature of a disc annulus is determined by the emergent flux at that radius, such that $T_{\rm eff}^4\propto F_{\rm bol}$. The emergent flux is the sum of viscous energy release within that annulus, $F_{\rm visc}\propto T_{\rm visc}^4$, and the X-rays reprocessed by the annulus, $F_{\rm irr}\propto T_{\rm irr}^4$. Hence the effective temperature is

$$T_{\rm eff}^4(R)=T_{\rm visc}^4(R)+T_{\rm irr}^4(R). \quad (1)$$

For fits to the UVOIR SED the model is particularly simple, as emission from the inner disc will not make a significant contribution; hence the inner disc radius is not important. The model is then parametrized by three values, the viscous and irradiation temperatures at the disc outer edge, $T_{\rm visc,out}$ and $T_{\rm irr,out}$, which determine the shape of the spectrum, and the normalization, which determines the overall flux level. We assume that the temperatures vary as

$$T_{\rm visc}(R)=T_{\rm visc,out}\left(\frac{R}{R_{\rm out}}\right)^{-3/4} \quad (2)$$

and

$$T_{\rm irr}(R) = T_{\rm irr,out}\left(\frac{R}{R_{\rm out}}\right)^{-3/7}, \quad (3)$$

following the references given above. After summing the local contributions from each disc annulus an overall normalization is applied to match the observed fluxes. The normalization used is defined as

$$\mathrm{Norm} = \left(\frac{R_{\rm disc}}{2\times10^{11}\,\mathrm{cm}}\right)^2\left(\frac{5\,\mathrm{kpc}}{d}\right)^2\cos i. \quad (4)$$

This normalization can inform us of *changes* in the outer disc radius, although measuring an absolute radius depends on the uncertain distance and inclination.

In principle stellar spectra could instead be used, but the smoothness of our derived SED (e.g. the absence of a Balmer jump) favours a blackbody spectrum, possibly indicating a close to isothermal disc atmosphere (even though the disc is not expected to be isothermal at larger optical depths).

This is obviously a very simple model, and as a theoretical model it has shortcomings. We will discuss the limitations in Section 5. In spite of these objections, variations on this model have been widely used (e.g. Shakura & Sunyaev 1973; Cunningham 1976; Vrtilek et al. 1990, 1991; Cheng et al. 1992; de Jong, van Paradijs & Augusteijn 1996; van Paradijs 1996; King, Kolb & Burderi 1996, and others) and it has the advantage of few free parameters. We feel that this simple description of the data is more valuable at this point than a more sophisticated model with more free parameters, especially as this provides a good fit to the observations. Conclusions can be drawn about the spectral evolution, although we must be somewhat cautious in interpreting the absolute parameters derived.

4.2 Model fits

The broad-band SEDs for all visits are shown in Fig. 4. We have fitted the disc model described above to each. We use only the *HST* data for the fit as the relative normalization of the not quite simultaneous UKIRT data is hard to establish without wavelength overlap. For each visit we have checked the overlaps between spectra and renormalized where necessary to ensure alignment. We also tried using the normalization of each spectrum as a free parameter of the fit, but we found this introduced too much freedom and fits were being produced with discontinuities at the boundaries between gratings. A fit with the normalizations fixed from the overlaps is somewhat poorer, but less prone to spurious parameters.

All fits were done by performing a grid search in the two temperatures and the normalization in order to estimate confidence regions. The formal χ^2 values for the fits are poor because the quality of the fit is restricted by limitations in the model and extinction curve used, rather than by statistical errors in the data. We therefore added an additional wavelength-independent systematic error to each point to give a best-fitting $\chi^2_{\rm R}$ of 1. These additional errors were represented as a fixed percentage (3–5 per cent) of the flux. The results of the fits (with $T_{\rm visc,out}$, $T_{\rm irr,out}$ and the normalization all allowed to vary freely) are summarized in Table 4 and the fits are plotted in Fig. 4. The confidence intervals quoted are projections of the three-parameter, 1σ confidence regions (Lampton, Margon & Bowyer 1976) estimated using the modified error prescription described above.

In general the fits are rather good, surprisingly so given the simplicity of the model. The main difficulties are in the IR, where the UKIRT data favour a flatter spectrum than the disc models provide, and in the UV, where the derived SEDs are sensitive to the exact shape of the extinction curve. The IR problem is also hinted at in some of the *HST* data, for example the red end of the 1999 November 6 SED rises somewhat with respect to the model. We will discuss this question further in Section 5.4.

4.3 Extension to X-ray energies

A natural progression from fitting the UVOIR SEDs is to also require that the disc models be consistent with the X-ray disc

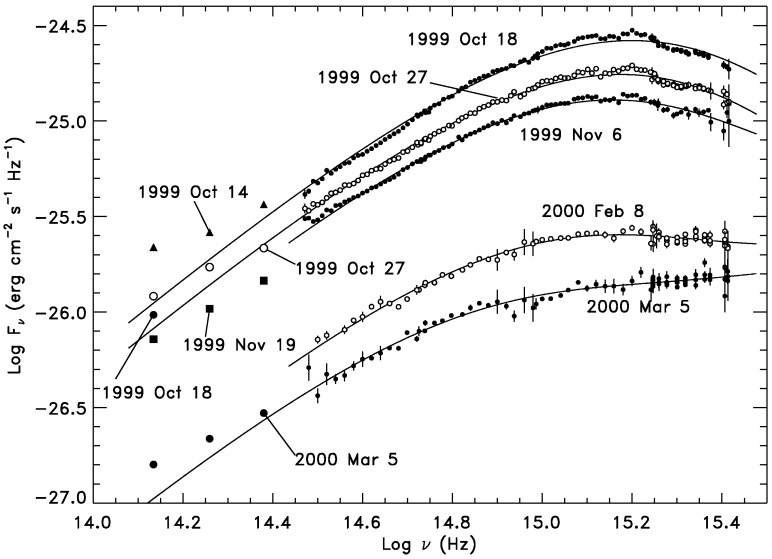

Figure 4. Evolution of the UVOIR SED through the outburst. Alternate *HST*/UKIRT visits are shown with open and filled circles for clarity. Additional UKIRT only visits are shown with triangles or squares. The best-fitting accretion disc model spectrum (fitted to the *HST* data only) is plotted on each one. The models are only extended into the IR for visits where we have UKIRT data. See text for details.

Table 4. Summary of results of fitting broad-band SEDs with accretion disc models. 1σ confidence intervals are given in brackets. These neglect uncertainties in the dereddening. The normalization in the last column is defined in equation 4.

Fit range (Å)	Date	$T_{\rm irr,out}$ (K)		$T_{\rm visc,out}$ (K)		Normalization	
1150–10200	1999 Oct 18	18500	(18300–18600)	100	(0–3600)	0.180	(0.176–0.185)
	1999 Oct 27	17500	(17400–17600)	200	(0–3600)	0.142	(0.139–0.145)
	1999 Nov 6	15900	(15500–16300)	5900	(4600–6700)	0.130	(0.126–0.135)
	2000 Feb 8	12700	(12100–13600)	8000	(7800–8100)	0.035	(0.032–0.038)
	2000 Mar 5	8300	(7300–9300)	8000	(7700–8200)	0.031	(0.027–0.035)
1660–10200	1999 Oct 18	20000	(19600–20200)	0	(0–6000)	0.152	(0.149–0.157)
	1999 Oct 27	18100	(16900–18500)	5200	(0–8400)	0.133	(0.129–0.140)
	1999 Nov 6	14700	(13600–15800)	8200	(6600–9000)	0.136	(0.129–0.143)
	2000 Feb 8	11400	(8700–13700)	8800	(7500–9300)	0.037	(0.032–0.044)
	2000 Mar 5	7800	(0–10400)	8100	(7700–8400)	0.031	(0.025–0.040)

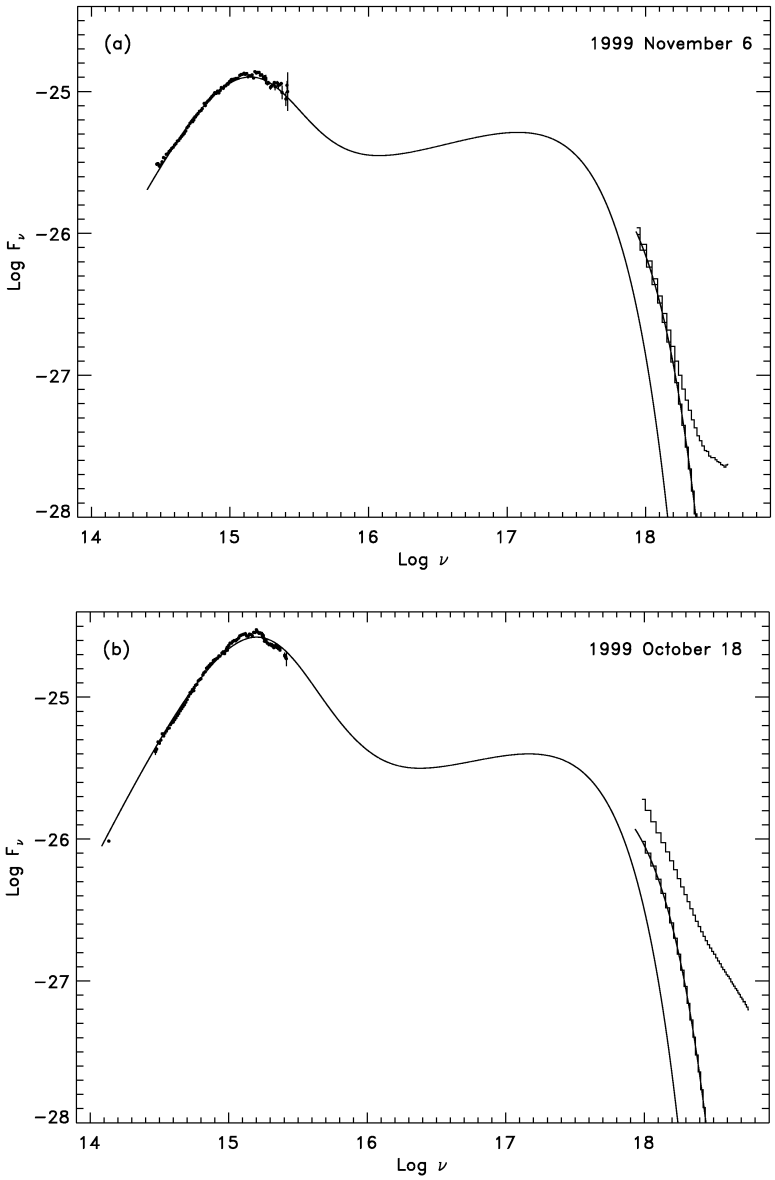

Figure 5. Full X-ray–IR SED for the two visits where an X-ray disc component was detected. *HST* and UKIRT points are indicated at left. Two *RXTE* spectra are given in each case; the upper is the total spectrum, the lower is the decomposed disc component. The solid line is the disc model SED; the short additional segment in the X-rays is the same modified by spectral hardening.

component, if seen. Our *RXTE* data do show disc components for the early epochs, 1999 October 18 and November 6. This component dominates in the latter visit. As the viscous temperature is also rather poorly constrained by the UVOIR data from the earlier visit, the November 6 data should provide the strongest test of consistency. To extend the model to X-rays we require an additional parameter, $r_{\rm in}$. In practice, given the uncertain distance and system parameters the data do not strictly constrain this, but rather $r_{\rm in}/r_{\rm out}$. Adjusting this ratio produces a one-parameter family of curves, with varying cut-off energies, one of which should match the X-ray disc component, assuming that a common model is applicable. There is some freedom to adjust the normalization of these curves by varying $T_{\rm visc}$ within the uncertainties allowed by the UVOIR fits. We find that this does appear to work, provided that the X-ray part of the SED is modified by spectral hardening (Shimura & Takahara 1995). We use a hardening factor of $f_{\rm col} = 1.7$ for both epochs, although this is a crude approximation as discussed below. Fig. 5(a) shows the X-ray and UVOIR data from November 6 with the best-fitting model. This model has $T_{\rm visc} = 5040$ K (consistent with the UVOIR fits), $r_{\rm in}/r_{\rm out} = 7.2 \times 10^{-5}$ and other parameters as given in Table 4. The bolometric disc luminosity of this model is $L_{\rm bol} \sim 1.6 \times 10^{38}$ erg s^{-1} for a distance $\sim$7.6 kpc (see Section 4.4), corresponding to $\sim$10 per cent of $L_{\rm Edd}$ for a 10-M$_\odot$ black hole. There will be a small additional contribution from the power-law component.

The same exercise can be carried out for the October 18 data, although here, the UVOIR constraints on $T_{\rm visc}$ are much weaker so there is more freedom to adjust this to fit the X-ray data. The best common fit is shown in Fig. 5(b), corresponding to $T_{\rm visc} = 3950$ K and $r_{\rm in}/r_{\rm out} = 3.9 \times 10^{-5}$. The low value of $T_{\rm visc}$ derived is almost consistent with the 1σ limit inferred from the UVOIR SED. The bolometric disc luminosity of this model is also $L_{\rm bol} \sim 1.6 \times 10^{38}$ erg s^{-1}, although for this visit the power-law component will make a much larger contribution, so the total luminosity is higher than for November 6.

Assuming a disc radius $\sim 0.9 \times 2 \times 10^{11}$ cm, consistent with likely parameters and a tidally truncated disc, then the implied inner radius at the first visit is $\sim$90 km. This is about $3R_{\rm Sch}$ for a 10-M$_\odot$ black hole, suggesting a disc extending to approximately the last stable orbit. Without a more reliable distance or system parameters, it is obviously not worth trying to be more precise. The derived inner radius is also sensitive to the choice of spectral hardening factor $f_{\rm col}$, and contrary to what is often assumed, this is unlikely to be constant; Merloni, Fabian & Ross (2000) suggest a range of 1.7–3 is plausible. The implied inner radius for the 1999 November 6 visit is somewhat larger than for October 18. Given the dramatic change in the spectral state, however, we cannot confidently say that this change is real (cf. Merloni et al. 2000); it could reflect a change in $f_{\rm col}$.

We therefore conclude that on those visits where X-ray disc emission is measured, it is consistent with a plausible extrapolation of the UVOIR fits, assuming a disc extending to around the last stable orbit. Therefore the disc models considered, modified for spectral hardening where necessary, and with additional non-thermal hard X-ray and IR contributions, represent an acceptable fit to the whole X-ray–IR SED.

4.4 The distance to the source

The normalization of the disc fits is dependent on the distance to the source, although obviously other factors also affect it. The normalization we used is defined by equation (4). To determine the distance we need to know the binary parameters. What we actually know is $P_{\rm orb} = (9.16 \pm 0.08)$ h and $f(M) = (7.4 \pm 1.1)$ M$_\odot$ (Filippenko & Chornock 2001). No eclipses have been reported, although an 0.4-mag ellipsoidal modulation appears to be present (Sanchez-Fernandez et al. 2000). The inclination is thus likely to be moderately large. Filippenko & Chornock (2001) found a best-fitting spectral type of G5, although they did not use earlier type templates. We can make a plausible distance estimate by assuming a typical black hole mass of $M_1 \sim 10$ M$_\odot$, a G5 companion mass of $M_2 \sim 1$ M$_\odot$ (Gray 1992), $P_{\rm orb} = 9.16$ h, $i \sim 60^\circ$ and a disc filling 90 per cent of the black hole's Roche lobe (i.e. tidally truncated) for the first visit with the largest normalization. We then derive a distance estimate of 7.6 kpc. Obviously the errors on this are large. To attempt to quantify these we perform a simple Monte Carlo simulation. We construct a population of binaries with randomly chosen parameters. We take a uniform black hole mass distribution of $M_1 = 5$–12 M$_\odot$ (Bailyn et al. 1998), a uniform companion mass distribution ($M_2 = 0.68$–1.12 M$_\odot$) corresponding to G0–G9 spectral type (Gray 1992), allowing for a possibly undermassive companion (Kolb, King & Baraffe 2001), a Gaussian period distribution of $P_{\rm orb} = (9.16 \pm 0.08)$ h and a uniform distribution in $\cos i = 0$–1. We then reject any binaries in which the central source is eclipsed and weight the remainder so as to produce a Gaussian mass-function distribution of $f(M) = (7.4 \pm 1.1)$ M$_\odot$. The resulting distribution of distance estimates then has a 95 per cent confidence range of 4.6–8.0 kpc, so we believe this is a reasonable estimate of the range of probable distances given the current uncertainty in the system parameters. Of course these estimates are model-dependent, and we have not accounted for further uncertainties introduced by assuming an extinction curve and $E(B-V)$ value, so a closer or further distance cannot confidently be ruled out. Also if the disc does not extend to the tidal truncation radius ($0.9r_{\rm lobe}$) at maximum then the distance would be reduced.

4.5 Physical parameters

We can now attempt to use the assumed binary parameters and our distance estimate to convert the viscous temperatures and normalizations derived into mass transfer rates, although there obviously will be large uncertainties in this process. The mass transfer rate, $\dot{M}$, is related to $T_{\rm visc}$ and the normalization by (see Frank et al. 1992 and equation 4)

$$\dot{M} = 4.54 \times 10^{-7} \left(\frac{M}{10\,{\rm M}_\odot}\right)^{-1} \left(\frac{T_{\rm visc}}{10^4\,{\rm K}}\right)^4 \left(\frac{d}{10\,{\rm kpc}}\right)^3 \times \left(\frac{\rm Norm}{\cos i}\right)^{-3/2} {\rm M}_\odot\,{\rm yr}^{-1}. \quad (5)$$

For the first two visits $T_{\rm visc}$ is not well defined, but $\dot{M}$ can be estimated for the other visits. Assuming $M = 10$ M$_\odot$, $d = 7.6$ kpc and $i = 60^\circ$, we derive $\dot{M} \sim 2.6 \times 10^{-8}$, 1.2×10^{-8} and 1.0×10^{-8} M$_\odot$ yr^{-1} for 1999 November 6, 2000 February 8 and 2000 March 5 respectively. Assuming a 10-M$_\odot$ black hole and an accretion efficiency of 10 per cent, the Eddington limited mass transfer rate is $\dot{M}_{\rm Edd} = 2.3 \times 10^{-7}$ M$_\odot$ yr^{-1}. Thus the November 6 observation corresponds to $\dot{M} \sim 0.1\dot{M}_{\rm Edd}$, as already estimated from the X-ray spectrum, while the later visits are lower, $\sim$5 per cent. These are reasonable numbers. The X-ray decay in this period is more dramatic than a factor of 2–3, but this will be amplified by the shifting of the X-ray spectrum out of the ASM bandpass.

For the 1999 November 6 visit it is also of interest to compare the irradiation temperature with the X-ray luminosity. As will be discussed in Section 5.3, some of the assumptions used deriving the exact irradiation temperature distribution are unjustified, and so it would not be appropriate to interpret the results in too much detail. A simple prescription has been advanced by Dubus et al. (1999), who write the irradiation temperature as

$$T_{\rm irr}^4 = C\frac{\dot{M}c^2}{4\pi\sigma R^2}, \qquad (6)$$

where a simple relation between $\dot{M}$ and L_X has been assumed. The parameter C encompasses our ignorance of the exact irradiation geometry; Dubus et al. (1999) use $C \sim 5\times10^{-4}$ for consistency with earlier results. Using our parameters derived for 2000 November 6 we obtain $C \sim 7.4\times10^{-4}$, in reasonable agreement with the value used by Dubus et al. (1999). This agreement is as good as can be expected given the uncertainty about many parameters.

5 DISCUSSION

5.1 Interpretation in the context of the disc instability model

The decrease in the normalizations given in Table 4 clearly suggest a systematic decrease in the projected disc area as the outburst decays (equation 4); as the distance and inclination are constant it must be the projected area which varies. We attribute this to changes in radius of the hot area of the disc, but changes in the projection arising from disc warping may also be involved (cf. Section 5.2). This could represent a change in the actual radius of the outer disc, but given the relatively large change seen it is more likely that it represents a cooling wave moving inwards through the disc. The spectrum would then be dominated by the inner hot disc; the outer disc is present but is much cooler and possibly optically thin, so would only make a weak contribution. King & Ritter (1998) have considered the evolution of an irradiated disc in a BHXRT. Their model interprets two kinds of decay behaviour – exponential and linear decays. During the exponential decay phase the whole disc is maintained in a hot state by X-ray irradiation and the exponential decay is caused by the draining of mass from the disc. During the linear decay phase a cooling wave moves inwards at a rate determined by the decreasing irradiation flux. In a typical short-period BHXRT such as XTE J1859+226, an exponential decay phase is followed by a linear decay; all of our observations took place during the exponential decay phase (Casares et al. 2000 report photometry indicating that the exponential decay phase lasted until 2000 May 30). None the less we see a significant decrease in hot disc area, suggesting that actually the disc is not all maintained in the hot state but that the cooling wave is allowed to propagate. Further, we see the irradiation temperature at the edge of the disc decreasing, suggesting that the cooling wave propagation is not controlled straightforwardly by the decreasing irradiation flux – neither the irradiation temperature, nor the combined effective temperature, is approximately constant at the edge of the hot disc. Our observations thus do not support the details of the model of King & Ritter (1998) in which a cooling front is completely inhibited.

If the decrease in normalization is due to the propagation of a cooling wave then the implied velocity is rather slow; $\sim1.5\times10^{11}$ cm over $\sim$140 d, corresponding to an average of only $\sim$6 cm s^{-1}. This is significantly below theoretical cooling wave velocities (in the absence of irradiation) of $\sim$1 km s^{-1} (Menou, Hameury & Stehle 1999; Cannizzo 2001). Given the presence of a secondary maximum (around day 140 in Fig. 1) which may involve restarting of the cooling wave such a simple calculation is naive. None the less, a discrepancy with theory is hard to avoid. It therefore seems likely that irradiation does slow the cooling wave significantly; in this respect we support King & Ritter (1998). The observations, however, suggest a modification of the model in which irradiation does not completely stop the cooling wave, but allows it to move slowly as the irradiating flux declines.

As noted earlier, given the uncertain extinction curve and simplistic local spectrum assumed, we should not interpret the temperatures described too literally. None the less it is worth noting that they do qualitatively make sense in the context of the disc instability model. In the later visits when irradiation is less strong, the inferred viscous temperatures at the edge of the hot disc, $\sim$8000 K, are close to that expected; the viscous temperature is the best indicator of the internal temperature of the disc, since irradiation will only ever be dominant in the surface layers (cf. Dubus et al. 1999). For $\alpha \sim 0.1$, $M_1 \sim 10\,{\rm M}_\odot$ and $R \sim 8\times10^{10}$ cm (assuming a first visit disc radius $\sim0.9\times2\times10^{11}$ cm and normalization $\propto R^2$), we expect a critical viscous effective temperature of $\sim$6600 K (Dubus et al. 1999). For the first two visits, however, the inferred viscous temperature is lower than this, and the weak dependence of the critical temperature on radius cannot resolve this discrepancy. It seems likely that the strong irradiation inferred at these epochs is stabilizing the disc at a radius larger than would be expected from viscous heating alone; as discussed by Dubus et al. (1999) strong irradiation is expected to reduce the critical temperature.

The evolution of the spectrum from irradiation-dominated to viscous-heating-dominated is a consequence of the weaker dependence of irradiation on radius ($\propto R^{-2}$) than the dependence of viscous heating ($\propto R^{-3}$). For a given irradiating flux and a large enough disc the outer part will be irradiation-dominated whereas the inner part is viscous-heating-dominated. Analogously, we would expect the edge of a large disc to be irradiation-dominated whereas the edge of a small disc will be dominated by viscous heating, assuming that the ratio of irradiating flux to $\dot{m}$ does not change dramatically.

5.2 Disc warping

A further factor that may come into play is warping of the disc. Dubus et al. (1999) have already invoked this as a possible mechanism to allow irradiation of the outer parts of a disc when it would otherwise be self-shielded. If warping is important then the irradiated area (and hence the normalization of the SED) may depend in a complex way on the warp geometry and changes in the normalization could indicate changes in this geometry rather than in the disc, or cooling front, radius. Such changes have previously been suggested to explain the light curves of another BHXRT with more unusual behaviour, GRO J1655−40 (Esin, Lasota & Hynes 2000). Ogilvie & Dubus (2001) have argued, however, that short-period BHXRTs with 'classic' fast-rise, exponential-decay (FRED) light curves, such as XTE J1859+226, are stable against radiation driven warping and that it will only be important for longer period systems (e.g. GRO J1655−40). Clearly the effect of a warp, if present, would be complex, and the observed spectrum may depend on the precession phase at the time of each observation. Also for a transient in outburst the warp is likely to be evolving as the outburst progresses. So although the development of a warp is unlikely to play a large role in a system such as XTE J1859+226,

we cannot observationally rule out this possibility that changes in warp geometry could contribute to the spectral changes we see.

5.3 Limitations of the model

Using blackbody local spectra is obviously an extreme simplification. It does work rather well, however, and the observed SEDs are almost as smooth as black bodies, in particular there is no detectable Balmer jump. This means that the obvious next refinement, to use stellar atmosphere spectra, as done by Vrtilek et al. (1990, 1991), would give a worse fit, since stars in the critical 10 000–20 000 K range, corresponding to the temperatures dominant in the disc spectrum, have strong Balmer absorption. A more sophisticated treatment would, therefore, require use of a model atmosphere generated specifically for an irradiated accretion disc atmosphere. Development of such models is underway (Hubeny 2002), but they are still in their infancy, depend on much uncertain physics and introduce many more free parameters. As a blackbody model does provide an acceptable fit to the data, we feel this is the most appropriate choice at this time.

There is also little justification for the irradiation temperature distribution assumed. The derivation of $T_{\rm irr} \propto R^{-3/7}$ assumes a vertically isothermal disc and cannot be correct. King, Kolb & Szuszkiewicz (1997) argue for a more realistic solution with the vertical temperature gradient accounted for. Their model gives $T_{\rm irr} \propto R^{-0.40}$, compared to $R^{-0.43}$ which we have used. The self-consistent treatment of Dubus et al. (1999) actually predicts that the outer disc should not be irradiated at all, contrary to observations (e.g. van Paradijs & McClintock 1995). Consequently additional factors such as disc warping and/or scattering of X-rays must be important and the true dependence of $T_{\rm irr}$ on radius is not known. Dubus et al. (1999) write the irradiation law as $T_{\rm irr} \propto CR^{-1/2}$, where the explicit radial dependence comes only from the inverse square law and additional unknown geometric factors are included in C, which they assume to be constant. In practice, however, the difference between assuming $R^{-0.5}$, $R^{-0.40}$ and $R^{-0.43}$ dependences is rather small. We have tested using all of these and our conclusions are not significantly affected by which we choose. The $R^{-3/7}$ is the intermediate relation and the most widely used to date, so is a reasonable approximation to choose.

Another simplification made is that a fixed fraction of incident X-rays are reprocessed into UVOIR emission, i.e. that the albedo is constant. This will not be true in the inner disc where the opacity may become dominated by electron scattering and a larger fraction of X-rays will be Compton reflected. In this inner region the disc will behave more like a mirror and reprocessing will be a less effective form of heating (A. R. King, private communication; A. C. Fabian, private communication). Shakura & Sunyaev (1973) give an approximate expression for the radius within which electron scattering will dominate, $R/3R_{\rm sch} \sim 6.3 \times 10^3 \dot{m}^{2/3}$, where $\dot{m}$ is the mass transfer rate in units of the critical (Eddington limited) rate. We have experimented with turning off irradiation within this radius in our model. For a typical BHXRT in outburst with $\dot{m} \sim 0.1$–1.0, the effect on the UVOIR SED is relatively modest, $\sim$10 per cent in the far-UV dropping rapidly with increasing wavelength. Consequently it will not be possible to disentangle this effect without a better extinction curve as it will distort the spectrum in a similar way to the far-UV rise.

5.4 The infrared spectrum

The infrared photometry suggests a flatter spectrum than an extrapolation of the disc models predicts. This is particularly prominent on the first UKIRT observation where the flattening in the K band appears quite pronounced. Brocksopp et al. (2002) have independently suggested that flat-spectrum synchrotron emission may be important in the IR in this source, and our results support their conclusion. In fact, another BHXRT, XTE J1118+480, shows a very convincing case for flat-spectrum synchrotron emission in the IR, and probably also in the optical (Hynes et al. 2000; Chaty et al., in preparation). It is interesting that the IR spectral slope does not change as it drops (except possibly for the first observation on the outburst rise). This would also fit with synchrotron, for example with the power of a jet changing but the spectrum staying about the same.

Of course an alternative explanation might be that the IR excess comes from the cool outer disc which we expect to be present, at least in the later visits. We would, however, expect this cool disc contribution to get stronger as the hot disc shrinks. The presence of the excess in all observations with *JHK* coverage does not fit with this, so the synchrotron interpretation seems more likely.

6 CONCLUSION

We have analysed the broad band UVOIR and X-ray spectra of XTE J1859+226 in outburst. We have found that all of the observations can be accounted for with a simple model accretion disc heated by internal viscosity and X-ray irradiation, if additional non-thermal components provide the flatter IR component and the X-ray power law. As the outburst declines we see a decrease in the normalization of the disc models and the irradiation temperature at the edge of the hot disc and an increase in the edge viscous temperature. We therefore see the outer disc change from being irradiation-dominated towards being viscous-heating-dominated with an accompanying decrease in the emitting area. We interpret the latter as evidence for a cooling wave; the transition from irradiative to viscous heating is qualitatively consistent with this interpretation. The evolution is not consistent with a cooling wave controlled by some fixed irradiation temperature, but appears to depend on a combination of irradiative and viscous heating.

ACKNOWLEDGMENTS

RIH thanks Guillaume Dubus for some interesting discussions on irradiation of accretion discs and Jim Pringle and Andrew King for constructive criticism of these results. RIH, CAH and SC acknowledge support from grant F/00-180/A from the Leverhulme Trust. This paper was based on observations made with the NASA/ESA *Hubble Space Telescope*, obtained at the Space Telescope Science Institute, which is operated by the Association of Universities for Research in Astronomy, Inc., under NASA contract NAS 5-26555. Support for proposal GO 8245 was provided by NASA through a grant from the Space Telescope Science Institute, which is operated by the Association of Universities for Research in Astronomy, Inc., under NASA contract NAS 5-26555.

Thanks to Tony Roman and Kailash Sahu at STScI for support. The United Kingdom Infrared Telescope is operated by the Joint Astronomy Centre on behalf of the UK Particle Physics and Astronomy Research Council. UKIRT Service observations were obtained thanks to override time, which was pre-approved in case of outbursting transients (U/98A/19), to be coordinated with our *HST* and *RXTE* observations. We thank John K. Davies who scheduled, coordinated, prepared and supervised the override

observations. We also thank Ian Smail and Glenn Morrison (Oct 13 observations), Rob J. Ivison (Oct 18), A. Adamson (Oct 27) and T. R. Geballe (Nov 19) who performed the mentioned observations and Ken Chambers for obtaining the last visit IR coverage during IfA time. This research has made use of the SIMBAD data base, operated at CDS, Strasbourg, France, the NASA Astrophysics Data System Abstract Service and quick-look results provided by the ASM/*RXTE* team.

REFERENCES

Bailyn C. D., Jain R. K., Coppi P., Orosz J. A., 1998, ApJ, 499, 367
Blades J. C., Wheatley J. M., Panagia N., Grewing M., Pettini M., Wamsteker W., 1988, ApJ, 334, 308
Brocksopp C. et al., 2002, MNRAS, in press
Cannizzo J. K., 2001, ApJ, 556, 847
Cardelli J. A., Clayton G. C., Mathis J. S., 1989, ApJ, 345, 245
Casali M. M., Hawarden T. G., 1992, UKIRT Newsl., 4, 33
Casares J., Rodriguez-Gil P., Zurita C., Shahbaz T., Charles P., Hynes R., Abbott T., Hakala P., 2000, IAU Circ. 7451
Chaty S. et al., 1999, IAU Circ. 7284
Cheng F. H., Horne K., Panagia N., Shrader C. R., Gilmozzi R., Paresce F., Lund N., 1992, ApJ, 397, 664
Cherepashchuk A. M., 2000, Space Sci. Rev., 93, 473
Cui W., Shrader C. R., Haswell C. A., Hynes R. I., 2000, ApJ, 535, L123
Cunningham C., 1976, ApJ, 208, 534
dal Fiume D. et al., 1999, IAU Circ. 7291
de Jong J. A., van Paradijs J., Augusteijn T., 1996, A&A, 314, 484
Dubus G., Lasota J.-P., Hameury J.-M., Charles P. A., 1999, MNRAS, 303, 139
Esin A. A., Lasota J. P., Hynes R. I., 2000, A&A, 354, 987
Filippenko A. V., Chornock R., 2001, IAU Circ. 7644
Fitzpatrick E. L., 1999, PASP, 111, 63 (F99)
Fitzpatrick E. L., Massa D., 1988, ApJ, 328, 734
Fitzpatrick E. L., Massa D., 1990, ApJS, 72, 163
Frank J., King A., Raine D., 1992, Accretion Power in Astrophysics. Cambridge Univ. Press, Cambridge, p. 77–79
Garnavich P., Quinn J., 2000, IAU Circ. 7388
Garnavich P. M., Stanek K. Z., Berlind P., 1999, IAU Circ. 7276
Gray D. F., 1992, The observation and analysis of stellar photospheres, 2nd edn. Cambridge Univ. Press, Cambridge
Hawarden T. G., Leggett S. K., Letawsky M. B., Ballantyne D. R., Casali M. M., 2001, MNRAS, 325, 563
Hubeny I., 2002, in Gänsicke B., Beuermann K., Reinsch K., eds, ASP Conf. Ser. Vol. 261, The Physics of Cataclysmic Variables and Related Objects. Astron. Soc. Pac., San Francisco, in press
Hynes R. I., Haswell C. A., 2001, in Livio M., ed., A Decade of HST Science, poster book. STScI, Baltimore (astro-ph/0008144)
Hynes R. I. et al., 1998, MNRAS, 300, 64
Hynes R. I., Mauche C. W., Haswell C. A., Shrader C. R., Cui W., Chaty S., 2000, ApJ, 539, L37
King A. R., Ritter H., 1998, MNRAS, 293, L42
King A. R., Kolb U., Burderi L., 1996, ApJ, 464, L127
King A. R., Kolb U., Szuszkiewicz E., 1997, 488, 89
Kolb U., King A. R., Baraffe I., 2001, MNRAS, 321, 544
Lampton M., Margon B., Bowyer S., 1976, ApJ, 208, 177
Leitherer C. et al., 2001, STIS Instrument Handbook, Version 5.1. STScI, Baltimore
Markwardt C. B., Marshall F. E., Swank J. H., 1999, IAU Circ. 7274
Menou K., Hameury J. M., Stehle R., 1999, MNRAS, 305, 79
Merloni A., Fabian A. C., Ross R. R., 2000, MNRAS, 313, 193
McCollough M. L., Wilson C. A., 1999, IAU Circ. 7282
Ogilvie G. I., Dubus G., 2001, MNRAS, 320, 485
Persson S. E., Murphy D. C., Krzeminski W., Roth M., Rieke M. J., 1998, AJ, 116, 2475
Pooley G. G., Hjellming R. M., 1999, IAU Circ. 7278
Sanchez-Fernandez C., Zurita C., Casares J., Shahbaz T., Castro-Tirado A., 2000, IAU Circ. 7506
Seaton M. J., 1979, MNRAS, 187, 73P
Shakura N. I., Sunyaev R. A., 1973, A&A, 24, 337
Shimura T., Takahara F., 1995, ApJ, 445, 780
Shrader C. R., Wagner R. M., Hjellming R. M., Han X. H., Starrfield S. G., 1994, ApJ, 434, 698
Tanaka Y., Shibazaki N., 1996, ARA&A, 34, 607
van Paradijs J., 1996, ApJ, 464, L139
van Paradijs J., McClintock J. E., 1995, in Lewin W. H. G., van Paradijs J., van den Heuvel E. P. J., eds, X-ray Binaries. Cambridge Univ. Press, Cambridge, p. 58
Vrtilek S. D., Raymond J. C., Garcia M. R., Verbunt F., Hasinger G., Kürster M., 1990, A&A, 235, 162
Vrtilek S. D., Penninx W., Raymond J. C., Verbunt F., Hertz P., Wood K., Lewin W. H. G., Mitsuda K., 1991, ApJ, 376, 278
Wagner R. M., Smith P. S., Schmidt G. D., Shrader C. R., 1999, IAU Circ. 7279
Wood A., Smith D. A., Marshall F. E., Swank J., 1999, IAU Circ. 7274

This paper has been typeset from a TEX/LATEX file prepared by the author.